JOURNAL OF AGRICULTURAL AND FOOD CHEMISTRY

Crocetin, Dimethylcrocetin, and Safranal Bind Human Serum Albumin: Stability and Antioxidative Properties

CHARALABOS D. KANAKIS,† PETROS A. TARANTILIS,† HEIDAR ALI TAJMIR-RIAHI,‡ AND MOSCHOS G. POLISSIOU*,†

Laboratory of Chemistry, Department of Science, Agricultural University of Athens, 75 Iera Odos, 11855 Athens, Greece, and Department of Chemistry-Biology, University of Québec at Trois-Rivières, TR (Québec) Canada G9A5H7

Crocetin (CRT) and dimethylcrocetin (DMCRT) are derived from crocins which are found in the stigmas of saffron (*Crocus sativus* L.), while safranal is the main component of saffron's essential oil. The aim of the present study was to examine their interaction with human serum albumin in aqueous solution at physiological conditions using constant protein concentration and various ligand contents. FT-IR and UV-visible spectroscopic methods were used to determine the ligands' binding mode, the binding constant, and the effects of ligand complexation on protein secondary structure. Structural analysis showed that crocetin, dimethylcrocetin, and safranal bind nonspecifically (H-bonding) *via* protein polar groups with binding constants of K_{crt} =2.05 (±0.30) × 10^3 M^{-1}, K_{dmcrt} = 9.60 (±0.35) × 10^4 M^{-1}, and K_{saf} = 2.11 (±0.35) × 10^3 M^{-1}. The protein secondary structure showed no major alterations at low ligand concentrations (1 μM), whereas at higher content (1 mM), decrease of α-helix from 55% (free HSA) to 43−45% and increase of β-sheet from 17% (free HSA) to 18−22% and random coil 7% (free HSA) to 10−14% occurred in the ligand−HSA complexes. The results point to a partial unfolding of protein secondary structure at high ligand content. The antioxidant activity of CRT, DMCRT, and safranal was also tested by the DPPH• antioxidant activity assay, and their IC_{50} values were compared to that of well-known antioxidants such as Trolox and butylated hydroxy toluene (BHT). The IC_{50} values of CRT and safranal were 17.8 ± 1 μg/mL and 95 ± 1 μg/mL, respectively, while the inhibition of DMCRT reached a point of 38.8%, which corresponds to a concentration of 40 μg/mL, and then started to decrease. The IC_{50} values of Trolox and BHT were 5.2 ± 1 μg/mL and 5.3 ± 1 μg/mL, respectively.

KEYWORDS: Human serum albumin; *Crocus sativus* L.; saffron; crocetin; dimethylcrocetin; safranal; protein; binding mode; binding constant; antioxidant activity; FT-IR; UV−vis spectroscopy

INTRODUCTION

Saffron is the commercial name of the dried stigmas of *Crocus sativus* L. flowers. The substances responsible for the characteristic quality of saffron are crocins, picrocrocin, and safranal. Crocins, glucosyl esters of crocetin, are uncommon water-soluble carotenoids and represent the yellow pigments of saffron. Picrocrocin is responsible for saffron's bitter taste. Safranal, the main component of the distilled essential oil of saffron, is a monoterpene aldehyde, responsible for its characterizric aroma (*1*). It is of interest that orally administered crocins are hydrolyzed to crocetin before or during intestinal absorption, and absorbed crocetin is partly metabolized to mono- and diglucoronide conjugates (*2*). Carotenoids play an important role in human health by acting as biological antioxidants, protecting cells and tissues from the damaging effects of free radicals and singlet oxygen (*3*, *4*). Carotenoids act as antioxidants by quenching singlet oxygen or free radicals that are formed during lipid oxidation (*5*−*8*). The antitumor activity of saffron and its components has been the subject of several recent reviews, and their potential pharmaceutical and medicinal applications are discussed in details (*9*−*11*). The induced chirality upon crocetin binding to human serum albumin and other serum albumins has been studied, but there is no information about the changes caused to the protein's secondary structure due to crocetin's binding (*12*, *13*). Human serum albumin (*14*) is the principal extracellular protein with a high concentration in blood plasma (40 mg/mL) (*15*, *16*) and due to its exceptional ability to interact with many organic and inorganic molecules make this protein an important regulator of intercellular fluxes, as well as the pharmacokinetic behavior of many drugs (*17*−*24*). Therefore, it was of interest to study the interaction of human serum albumin with crocetin, dimethylcrocetin, and safranal in aqueous

* To whom correspondence should be addressed. Phone: +30-210-529 4241. Fax: +30-210-529 4265. E-mail: mopol@aua.gr.
† Agricultural University of Athens.
‡ University of Québec at Trois-Rivières.

10.1021/jf062638l CCC: $37.00
Published on Web 01/09/2007

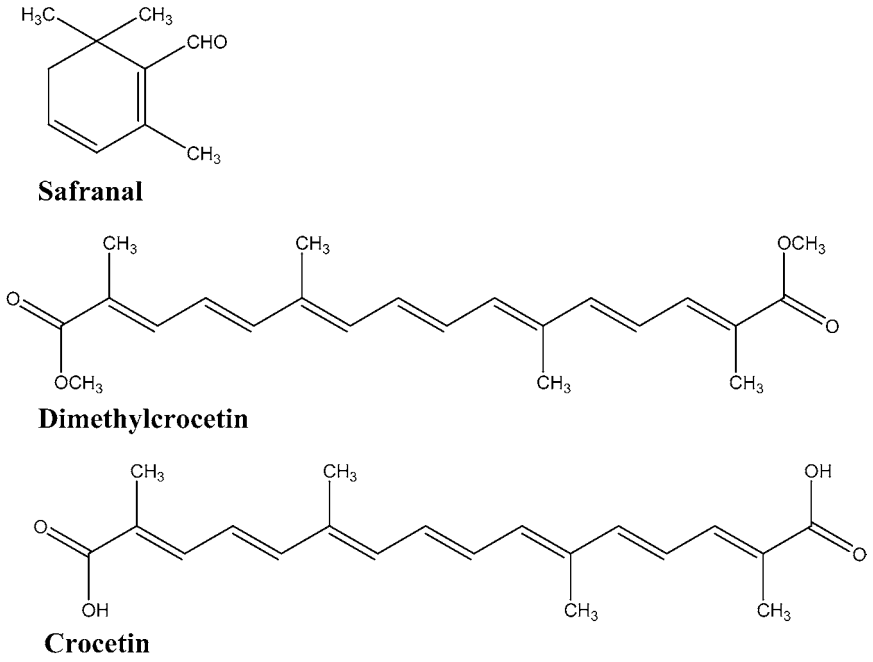

Figure 1. Chemical structure of safranal, dimethylcrocetin, and crocetin.

solution and to examine the effects of these biomolecules' complexation on protein stability and secondary structure.

We now report the FT-IR and UV-visible spectroscopic results on the interaction of human serum albumin with crocetin, dimethylcrocetin, and safranal (**Figure 1**) in aqueous solution at physiological conditions with constant protein concentration (0.15 mM for FT-IR and 0.015 mM for UV−vis measurements) and various ligand contents (1 μM to 1 mM for FT-IR and 0.01 mM to 1 mM for UV−vis measurments). The antioxidant activity of the ligands evaluated by the DPPH• method together with structural information regarding the ligands' binding mode, binding constants, and the effects on the protein's stability and secondary structure are provided here.

MATERIALS AND METHODS

Materials. Human serum albumin fraction V, isophorone (97%), and 2,2-diphenyl-1-picrylhydrazyl (DPPH•) (90%) were purchased from Sigma. Trolox (97%) was purchased from Aldrich, butylated hydroxy toluene (BHT) from BDH, and safranal (75%) from Fluka. Other chemicals were of reagent grade and used without further purification. Stigmas of pure red Greek saffron were kindly supplied by the "Cooperative of Saffron, Krokos Kozanis".

Preparation of Crocetin (CRT). Five grams of *Crocus sativus* L. stigmas was purified from their essential oil after repeated extractions using petroleum spirit and diethyl ether (BHT free). The extractions took place in an ultrasound water bath (Sonorex, Super RK 255H type, 300 × 150 × 150 mm internal dimensions) at the fixed-frequency of 35 kHz (indirect sonication). The temperature of the sonicated water was 25 °C. Crocetin was prepared from an aqueous extract of the stigmas by alkaline hydrolysis (20 mL of 2 N KOH) and acidification (20 mL of 1 N H_2SO_4). Crocetin was purified by repeated extractions (at least three times) using methanol. Additional purification was obtained when crocetin (red powder) was dissolved in pyridine, which in turn was evaporated to dryness using a rotavapor. The purity and structure of the isolated crocetin was analyzed by FT-IR, and the results were in total agreement with those reported in the literature (*25*).

Preparation of Dimethylcrocetin (DMCRT). Five grams of *Crocus sativus* L. stigmas was purified from their essential oil following the procedure described for the preparation of CRT. DMCRT was synthesized from a methanol extract of *Crocus sativus* L. stigmas by alkaline catalysis (20 mL methanolic solution of 2 N KOH) and purified by extraction with dichloromethane. The dichloromethane extracts were evaporated to dryness using a rotavapor, and dimethylcrocetin was obtained in powder form. The purity and structure of the dimethylcrocetin was confirmed by FT-IR, and the results were in total agreement with those reported in the literature (*25*).

Measurement of Antioxidant Activity. *DPPH• Free Radical Antioxidant Activity of Safranal.* The antioxidant activity of safranal was evaluated by the DPPH• assay (*26*). Fifty microliters of various concentrations of safranal was added to 5 mL of a 0.004% methanol solution of DPPH•. After a 60 min incubation period at room temperature, the absorbance was read at 517 nm on a Jasco UV-visible V-550 spectrophotometer. Inhibition free radical DPPH• in percent (inhibition %) was calculated in the following way:

$$\text{inhibition } \% = [(A_{\text{control}} - A_{sample})/A_{\text{control}}] \times 100$$

where A_{control} is the absorbance at 517 nm of the control reaction (containing all reagents except the test compound) and A_{sample} is the absorbance at 517 nm containing the test compound. The concentration of safranal providing 50% inhibition (IC_{50}) was calculated from the graph plotted inhibition percentage against safranal concentration (μg/mL) (**Figure 2**). The antioxidant activity tests were carried out in triplicate.

DPPH• Free Radical Antioxidant Activity of DMCRT and CRT. The antioxidant activity of DMCRT and CRT was evaluated by the DPPH• assay (*26*), but instead of measuring the absorbance at 517 nm, the UV−vis spectrum of the solution containing the saffron carotenoids and the DPPH• was recorded on a Jasco UV−vis V-550 spectrophotometer.

The structure of the carotenoids provides a chromophoric system which leads to interference in the DPPH• method currently using the 517 nm wavelength as described above. In this work the value of the absorbance at this wavelength was due to saffron's carotenoids and to the DPPH•. Because of this interference the calculation of the inhibition of DPPH•, using the above-described procedure for safranal, was false. Moreover, since the higher the percentage of DPPH• remaining, the lower is the radical-scavenging activity of the carotenoid, all the measurements of the antioxidant activity using the procedure described for safranal were underestimated. To avoid this interference, some authors tested the antioxidant activity of carotenoids by measuring the absorbance at 580 nm (*27*). Still in our case the interference described above remained. For this reason we used the curve-fitting procedure using the GRAMS/AI Version 7.01 software from Galactic Industries Corporation. By means of the second derivative in the spectral region 360−700 nm, five major peaks were resolved. The above spectral region

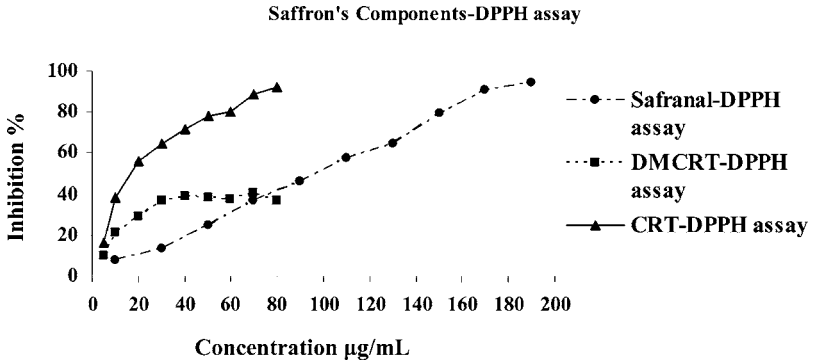

Figure 2. Inhibition (%) against various concentrations of safranal, DMCRT, and CRT used in the DPPH• test. Results are means of three different measurements.

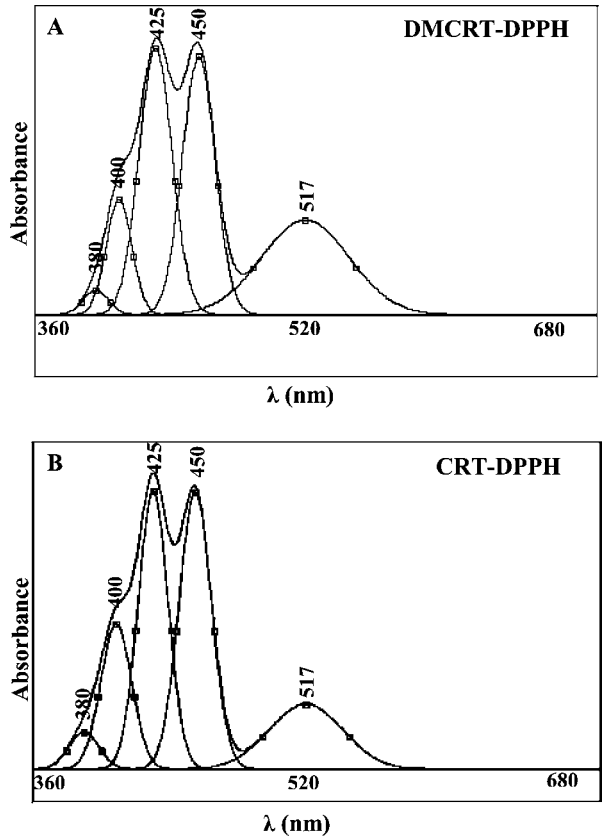

Figure 3. Curve-fitted in the spectral region 360–700 nm for the peaks at 380 nm, 400, 425, and 450 nm corresponding to the carotenoids while the peak at 517 nm corresponds to the DPPH•.

was deconvoluted by the curve-fitting method with the Levenberg−Marquadt algorithm, and the peaks at 380 nm, 400, 425, and 450 nm correspond to the carotenoids while the peak at 517 nm corresponds to the DPPH•. The area of the DPPH• peak was measured with the Gaussian function (**Figure 3**). Inhibition free radical DPPH• in percent (inhibition %) was calculated in the following way:

$$\text{inhibition } \% = [(B_{\text{control}} - B_{\text{sample}})/B_{\text{control}}] \times 100$$

where B_{control} is the area of the DPPH• peak of the control reaction (containing all reagents except the test compound) and B_{sample} is the area of the DPPH• peak containing the test compound. The concentration of the carotenoid providing 50% inhibition (IC_{50}) was calculated from the graph plotted inhibition percentage against carotenoid concentration (μg/mL) (**Figure 2**). The antioxidant activity tests were carried out in triplicate.

Preparation of Ligand−HSA Stock Solutions. Human serum albumin was dissolved in aqueous solution (20 mg/mL or 0.3 mM) containing potassium dihydrogen phosphate buffer 0.1 M (pH 7.0). The protein concentration was determined spectrophotometrically using the extinction coefficient of 36 500 M^{-1} cm^{-1} at 280 nm (*28*). In this study, HSA did not have its fatty acids removed, thus being in a situation closer to what which occurs *in vivo*. Indeed, under normal physiological conditions, between 0.1 and 2 fatty acid molecules are bound to the albumin (*20*). The carotenoids and safranal solutions (0.002 mM to 2 mM) were prepared in ethanol/water mixture (25/75%). In the final step, carotenoids and safranal solution was added dropwise to the protein solution with constant stirring to ensure the formation of homogeneous solution and to attain the final ligand (carotenoids and safranal) concentrations of 0.001, 0.01, 0.1, and 1 mM with a final protein concentration of 0.15 mM (or with ligand/protein molar ratios of 0.0067, 0.067, 0.67, and 6.7) for infrared measurements.

FT-IR Spectroscopic Measurements. Infrared spectra were recorded on a Nicolet Magna 750 FT-IR spectrophotometer (DTGS detector, Ni-chrome source and KBr beamsplitter) with a total of 100 scans and resolution of 4 cm^{-1}, using AgBr windows. Spectra were collected after 1 h of incubation of HSA with the ligands and measured in triplicate (three individual samples with the same protein and drug concentrations) on hydrated films. The difference spectra [(protein solution) − (protein solution + ligand solution)] (*29*) were generated using the polypeptide antisymmetric and symmetric C−H stretching bands (*30*), located at 2900−2800 cm^{-1} as internal standard. Details regarding infrared spectral treatment are given in our recent publication (*31*).

Determination of the Protein Secondary Structure. Analysis of the secondary structure of HSA and its ligand complexes was carried out on the basis of the procedure previously reported (*32*). The protein secondary structure is determined from the shape of the amide I band, located around 1650−1660 cm^{-1}. The FT-IR spectra were smoothed, and their baselines were corrected automatically using the built-in software of the spectrophotometer (OMNIC ver. 3.1). Thus the root-mean square (rms) noise of every spectrum was calculated. By means of the second derivative in the spectral region 1600−1700 cm^{-1}, seven major peaks for HSA and the complexes were resolved. The above spectral region was deconvoluted by the curve-fitting method with the Levenberg−Marquadt algorithm, and the peaks corresponding to α-helix (1656−1658 cm^{-1}), β-sheet (1614−1638 cm^{-1}), turn (1660−1677 cm^{-1}), random coil (1640−1648 cm^{-1}), and β-antiparallel (1680−1692 cm^{-1}) were adjusted and the area was measured with the Gaussian function. The area of all the component bands assigned to a given conformation were then summed up and divided by the total area (*33*). The curve-fitting analysis was performed using the GRAMS/AI Version 7.01 software of the Galactic Industries Corporation.

Absorption Spectroscopy. The UV−vis spectra were recorded on a Jasco UV−vis V-550 spectrophotometer with final carotenoids and safranal concentrations of 0.01 mM to 1 mM and a constant protein concentration of 0.015 mM.

The values of the binding constants *K* were obtained from the optical absorption at 280 nm according to the method described by Stephanos

Table 1. IC_{50} Values (μg/mL) of Safranal and Crocetin (CRT)

substances tested	IC_{50} (1 h incubation)[a]
safranal	95 ± 1 μg/mL
CRT	17.8 ± 1 μg/mL
Trolox	5.2 ± 1 μg/mL
BHT	5.3 ± 1 μg/mL

[a] Results are means of three different measurements.

J (*34*, *35*) where he described the binding of various ligands to hemeoglobin. For weak binding cases, the data were treated using linear reciprocal plots based on

$$\frac{1}{A - A_0} = \frac{1}{A_\infty - A_0} + \frac{1}{K(A_\infty - A_0)} \cdot \frac{1}{C_{\text{ligand}}} \quad (1)$$

where, A_0 is the absorption of HSA at 280 nm in the absence of ligand, A_∞ is the final absorption of the ligated protein, and A is the recorded absorption at different ligand concentrations.

Thus, the double reciprocal plot of $1/(A - A_0)$ vs $1/C_{\text{ligand}}$ is linear and the binding constant (K) can be estimated from the ratio of the intercept to the slope (*34*, *35*).

RESULTS AND DISCUSSION

Antioxidant Activity. The results of the DPPH• assay for DMCRT and CRT are shown in **Figure 2**. The antioxidant activity of DMCRT increased with concentration up to 40 μg/mL, showing an inhibition percentage for the DPPH• of 38.8% and starting to decrease at higher concentrations. This might be explained by the fact that at higher concentrations DMCRT acts as an oxygen-carrying agent (*36*). This oxygen-dependent step is often referred to as pro-oxidant effect since it theoretically could generate more radicals than it consumes (*37*). The same resulted for crocins when they were tested for their antioxidant activity by Pham et al. (*8*), and it is in agreement with our results of the antioxidant activity of crocins using the DPPH• assay with the curve-fitting method (unpublished data).

As shown in **Figure 2**, free radical scavenging activity of CRT was superior to DMCRT (CRT $IC_{50} = 17.8 \pm 1$ μg/mL, **Table 1**). The reason for that are the structural features of the two carotenoids as described by Jiménez-Escrib et al. (*27*). In the case of DMCRT and CRT the length of the conjugated double bonds is the same. The difference between the two carotenoids is the presence of the hydroxyl moiety of the carboxylic group on each of the termini of the unsaturated hydrocarbon chain in the case of CRT and in the case of DMCRT the presence of one methyl ester group on each of the termini of the unsaturated hydrocarbon chain. According to Roginsky et al. (*38*), the DPPH• test is based on the capability of the stable free radical 2,2-diphenyl-1-picrylhydrazyl to react with H-donors such as OH of carboxylic groups. The presence of OH of the carboxylic groups in CRT makes it more effective to react with DPPH•. In the case of DMCRT, as we explained above, the antioxidant activity reached a certain point and then started to decrease, and this behavior was also observed for other carotenoids too (*37*). This did not happen in the case of CRT. The antioxidant activity of CRT increased as the concentration increased.

Safranal is a monoterpene aldehyde and is the main component of saffron's essential oil. Its free radical scavenging activity is shown in **Figure 2**. It has lower antioxidant activity (safranal $IC_{50} = 95.0 \pm 1$ μg/mL, **Table 1**) than CRT. Comparing the antioxidant activity of safranal with that of DMCRT, it can be seen that for concentrations up to 40 μg/mL, DMCRT showed greater antioxidant activity (inhibition % = 38.8%) than that of safranal (inhibition % = ~20%).

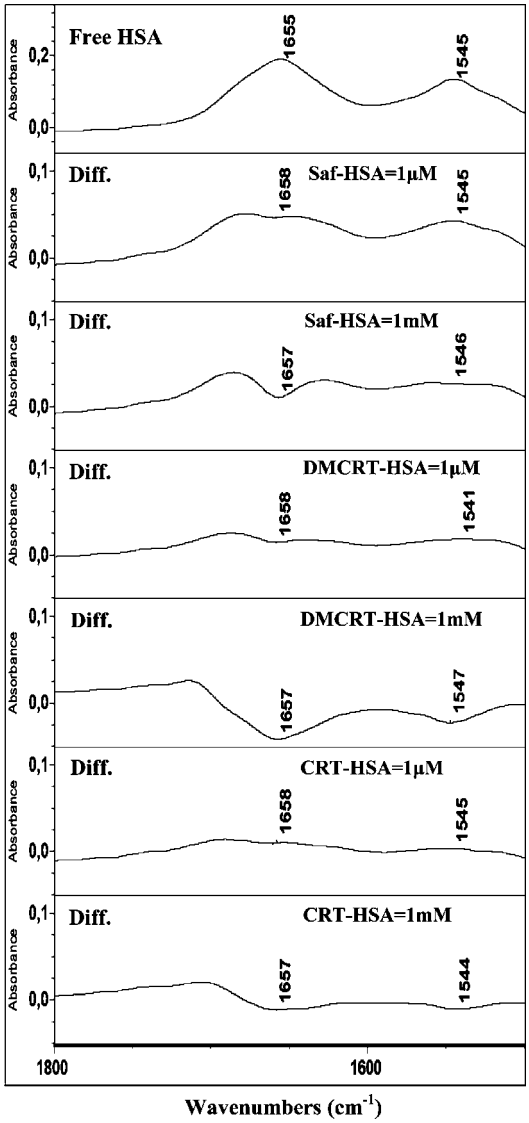

Figure 4. FT-IR spectra of hydrated film for the free HSA (top first curve) and difference spectra for ligand–HSA adducts (bottom six curves) in the region of 1800–1500 cm^{-1} with different ligand concentrations.

Table 1 shows the IC_{50} values of CRT, safranal, Trolox, and BHT. As can be seen, saffron's components in general showed lower antioxidant activity than that of Trolox and BHT and especially safranal, but the antioxidant activity of CRT is closer to that of BHT and Trolox. Thus saffron's carotenoids are more effective than safranal. However, the synergistic effect of all the bioactive constituents gives to saffron spice a significant antioxidant activity.

FTIR Spectra of Crocetin, Dimethylcrocetin, and Safranal Adducts with HSA. Evidence regarding crocetin, dimethyllcrocetin, and safranal−HSA complexation comes from infrared spectroscopic results. Since there was no major spectral shifting for the protein amide I band at 1655 cm^{-1} (mainly C═O stretch) and amide II band at 1545 cm^{-1} (C−N stretching coupled with N−H bending modes) (*24*, *32*), upon ligand interaction, the difference spectra [(protein solution) − (protein solution + ligand solution)] (*29*) were obtained, in order to monitor the intensity variations of these vibrations, and the results are shown in **Figure 4**. Similarly, the infrared self-deconvolution with second derivative resolution enhancement and curve-fitting

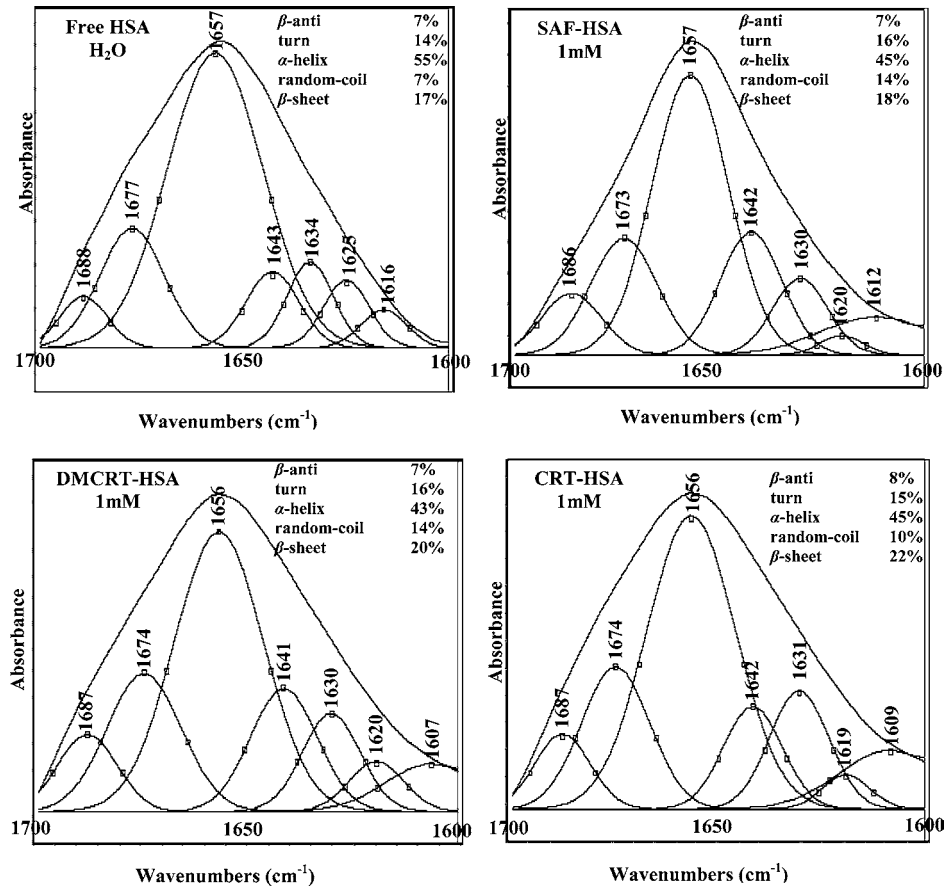

Figure 5. Curve-fitted amide I region (1700–1600 cm^{-1}) with secondary structure determination of the free HSA and its ligand complexes in aqueous solution with 1 mM ligand concentration and final HSA content 0.15 mM. The percentages of turns, random, α-helix, parallel β-sheet, and antiparallel (β-anti) structures were calculated as the ratio of the corresponding peak areas to the total of all seven amide I peaks.

Table 2. Secondary Structure Analysis for the Free HSA and Its Safranal (SAF), Dimethylcrocetin (DMCRT), and Crocetin (CRT) Complexes in Aqueous Buffer at pH 7.0 with Different Ligand Concentrations and Final Protein Content 0.15 mM (at 25 °C)

amide I components (cm^{-1})	free HSA (%)	SAF, 1 μM (%)	SAF, 1 mM (%)	DMCRT, 1 μM (%)	DMCRT, 1 mM (%)	CRT, 1 μM (%)	CRT, 1 mM (%)
1692–1680 β-anti	7 ± 2	7 ± 1	7 ± 2	5 ± 1	7 ± 2	6 ± 1	8 ± 1
1680–1660 turn	14 ± 1	11 ± 1	16 ± 1	14 ± 1	16 ± 1	14 ± 1	15 ± 1
1660–1650 α-helix	55 ± 1	53 ± 1	45 ± 1	53 ± 1	43 ± 1	55 ± 1	45 ± 1
1648–1641 random coil	7 ± 1	10 ± 1	14 ± 2	11 ± 1	14 ± 1	9 ± 1	10 ± 1
1640–1610 β-sheet	17 ± 1	19 ± 1	18 ± 1	17 ± 1	20 ± 1	16 ± 1	22 ± 1

procedures (*32*) were used to determine the protein secondary structures in the presence of crocetin, dimethylcrocetin, and safranal, and the results are presented in **Figure 5** and **Table 2**.

At low ligand concentration (1 μM), no major changes were observed for the protein amide I and amide II bands at 1655 and 1545 cm^{-1}, respectively (**Figure 4**, diff., 1 μM). However, at high ligand content (1 mM) strong negative features were observed at 1657 cm^{-1} and 1547−1544 cm^{-1} due to the amide I and amide II band intensity changes (**Figure 4**, diff., 1 mM). The loss of intensity of the amide I band and amide II band are due to interactions of crocetin, dimethylcrocetin, and safranal with the protein's C═O and C−N groups at high ligand concentration. The interactions of these ligands with the protein C−N group are also evident from the shift of the amide A band at 3368 cm^{-1} (peptide N−H stretching mode) (*24*) toward a higher frequency at 3372 cm^{-1}, upon ligand complexation (spectra not shown). The loss of intensity of the amide I band at 1655 cm^{-1} is also due to the alterations of the protein secondary structure, which will be discussed below.

A quantitative analysis of the protein secondary structure for the free HSA and its ligand complexes in H_2O is given in **Figure 5** and **Table 2**. The free protein contained major α-helix 55 ± 1%, β-sheet 17 ± 1%, random coil 7 ± 1%, turn structure 14 ± 1%, and β-antiparallel 7 ± 2% (**Figure 5** and **Table 2**). The β-sheet structure is composed of three components at 1616 cm^{-1} (inter β-strand), 1625 cm^{-1} (intra β-strand), and 1634 cm^{-1} (hydrated β-strand) that are consistent with the recent spectroscopic studies of the human serum albumin (*39*−*42*). Upon crocetin, dimethylcrocetin, and safranal complexation, no major alterations of protein conformation were observed at low ligand

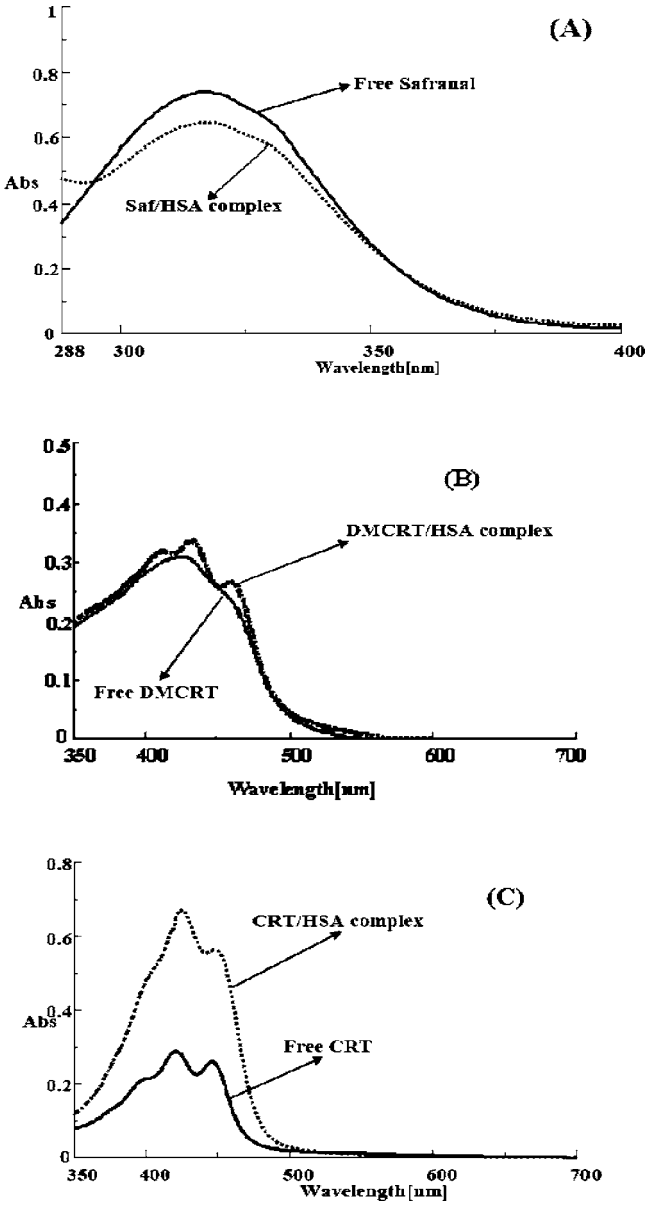

Figure 6. UV–visible spectral characteristics of ligands and their HSA adducts for safranal at 317 nm, DMCRT at 426 nm, and CRT at 421 nm with final HSA concentration of 0.015 mM, CRT content of 0.05 mM, safranal 0.1 mM, and DMCRT 1 mM.

concentration (1 μM), while at high ligand content the α-helix reduced from 55% to 43−45%, while the β-sheet increased from 17% to 18−22% (**Table 2**, 1 mM). The decrease in α-helix and increase in β-sheet is due to a partial protein unfolding at high ligand concentration. Analogous changes in the conformation of protein's secondary structure were observed in recent papers. Xie et al. (*43*) demonstrated the interaction between human serum albumin and morin, where they observed that α-helix and β-sheet structures tended to diminish with the increase in drug concentrations. Li et al. (*44*) studied the interaction of human serum albumin with formononetin. They observed major perturbations to HSA secondary structure upon formononetin interaction. Kanakis et al. (*45*) studied the binding of flavonoids to HSA. In their study the protein's secondary structure showed major alterations at high flavonoid content. A major decrease of α-helix and increase of β-sheet and β-anti occurred. Ahmed Ouamer et al. (*46*) observed alterations in protein conformation such as decrease of α-helix and increase of β-structure when chlorophyll and chlorophyllin bind to HSA.

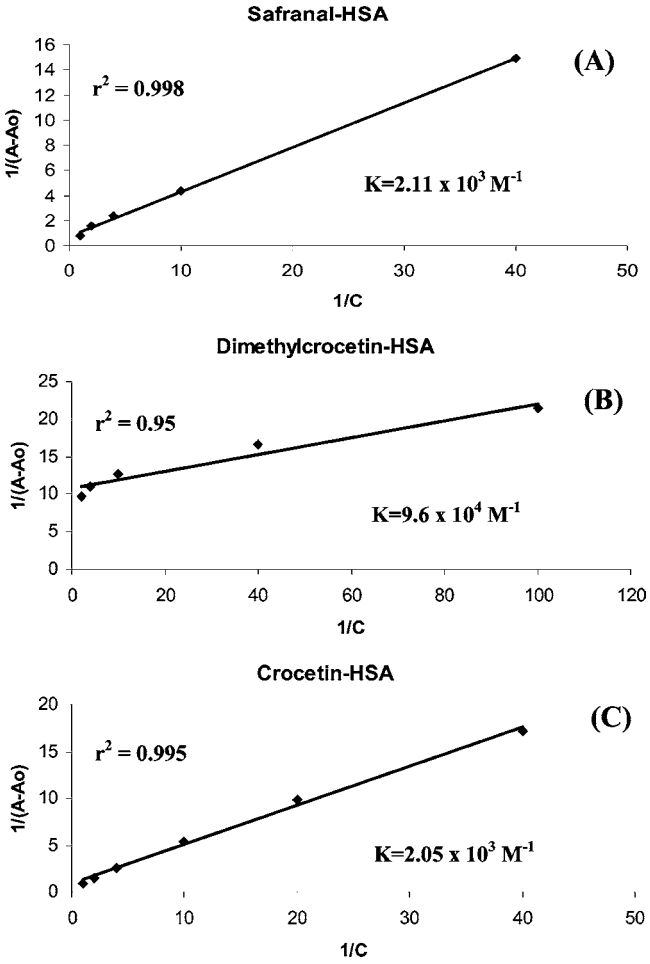

Figure 7. Plot of $1/(A - A_0)$ vs $1/C_{ligand}$ concentration for HSA and its ligand adducts, where A_0 is the initial absorption band of free HSA (280 nm), and A is the recorded absorption at different pigment concentrations (0.01 to 1 mM) and final HSA content of 0.015 mM.

The carotenoids and safranal solutions were prepared in ethanol/water mixture (25/75%) as it is described in Materials and Methods. It should be noted that 25% ethanol does not affect protein structure, while higher ethanol content (>50%) can alter protein structure. Shan-Yan Lin et al. (*47*) stated that after ethanol treatment the percentages of α-helix and β-sheet increased. In our case and especially in the presence of low ligand concentration (1 μM) the percentages of α-helix and β-sheet ranged from 53 to 55% and 16−19%, respectively. These values are very close to that of free HSA. So the alterations of protein conformation (high ligand concentration, 1 mM) are due to the presence of ligands.

UV-Visible Spectra and Stability of Ligand−HSA Adducts. The UV−vis spectra of the free crocetin, dimethylcrocetin, and safranal with their HSA complexes are shown in **Figure 6**. The band maximum of the free safranal at 317 nm decreased (hypochromic effect), but no major red shifting occurred (**Figure 6A**). The band maximum of dimethylcrocetin at 426 nm increased its intensity and a red shift from 426 to 433 nm occurred (**Figure 6B**). Similalry, the crocetin band at 421 nm increased its intensity upon protein complexation and a red shift from 421 to 425 nm also occurred (**Figure 6C**). The increase of intensity of UV−vis bands is due to major ligand−protein interaction at protein surface, which does not limit the mobility of ligand around HSA molecule. The decrease in intensity of the safranal band maximum at 317 nm observed upon HSA binding can be attributed to the smaller size of

safranal (with respect to crocetin and dimethylcorecetin), allowing major ligand penetration inside the protein molecule, which limits the safranal mobility. Safranal absorbs energy from the incident light, energy that is dispersed by molecular movements in the solvent. When safranal penetrates inside the protein molecule, safranal's movement is restricted by the structure of HSA. This loss of movement limits the amount of energy that can be dissipated, causing a decrease in absorption capability. However, the increase in intensity of the crocetin and dimethylcrocetin band maxima is attributed to the ligand external binding on the protein surface causing the opposite effect (increase of intensity) in comparison with safranal (*48*).

The binding constants of ligand−HSA complexes were calculated as described in Materials and Methods. The double reciprocal plot of pigment concentrations versus protein absorption is shown in **Figure 7**. The overall binding constants for crocetin, dimethylcrocetin, and safranal−protein adducts were estimated to be $K_{crt} = 2.05\ (\pm 0.30) \times 10^3\ M^{-1}$, $K_{dmcrt} = 9.60\ (\pm 0.35) \times 10^4\ M^{-1}$, and $K_{saf} = 2.11\ (\pm 0.35) \times 10^3\ M^{-1}$ (**Figure 7**). The binding constants calculated here show a weak ligand−protein interaction with respect to other strong ligand−protein complexes like monoclonal antibodies with binding constants from $10^7\ M^{-1}$ to $10^{10}\ M^{-1}$ (*49*). It is worth noting that natural products showed binding constants which are in order of magnitude smaller than the $10^7\ M^{-1}$ to $10^{10}\ M^{-1}$. Flavonoids display binding constants in the range $1-15 \times 10^4\ M^{-1}$ (*50*). Zsila et al. (*51*) demonstrated that the binding constant of quercetin was $1.46 \times 10^4\ M^{-1}$ while Kanakis et al. (*45*) showed that the binding constants for quercetin, kaempferol, and delphinidin were $1.4 \times 10^4\ M^{-1}$, $2.6 \times 10^5\ M^{-1}$, and $4.71 \times 10^5\ M^{-1}$, respectively.

LITERATURE CITED

(1) Kanakis, C. D.; Daferera, D. J.; Tarantilis, P. A.; Polissiou, M. G. Qualitative Determination of Volatile Compounds and Quantitative Evaluation of Safranal and 4-Hydroxy-2,6,6-trimethyl-1-cyclohexene-1-carboxaldehyde (HTCC) in Greek Saffron. *J. Agric. Food Chem.* **2004**, *52*, 4515−4521.

(2) Asai, A.; Nakano, T.; Takahashi, M.; Nagao, A. Orally administered crocetin and crocins are absorbed into blood plasma as crocetin and its glucuronide conjugates in mice. *J. Agric. Food Chem.* **2005**, *53*, 7302−7306.

(3) Polozza, P.; Krinsky, N. I. Antioxidant effects of carotenoids. *in vivo* and *in vitro.* An Overview. *Methods Enzymol.* **1992**, *213*, 403−420.

(4) Edge, R.; McGrevey, D. J.; Trusxott, T. G. The carotenoids as antioxidants. A review. *J. Photochem. Photobiol. B Biol.* **1997**, *41*, 189−200.

(5) Mortensen, A.; Skibsted, L. H. Importance of carotenoids structure in radical-scavenging reactions. *J. Agric. Food Chem.* **1997**, *45*, 2970−2977.

(6) Matheson, I. B. C.; Rodgers, M. A. J. Crocetin, a water soluble carotenoids monitor for singlet molecular oxygen. *Photochem. Photobiol.* **1982**, *36*, 1−4.

(7) Liebler, D. C.; Mcclure, T. D. Antioxidant reactions of beta-carotene: Identification of carotenoid-radical adducts. *Chem. Res. Toxicol.* **1996**, *9*, 8−11.

(8) Pham, T. Q.; Cormier, F.; Farnworth, E.; Tong, V. H.; Van Calsteren, M. R. Antioxidant properties of crocin from *Gardenia jasminiodes* Ellis and study of the reactions of crocin with linoleic acid and crocin with oxygen. *J. Agric. Food Chem.* **2000**, *48*, 1455−1461.

(9) Giaccio, M. Crocetin from saffron: An active component of an ancient spice. *Crit. Rev. Food Sci. Nutrit.* **2004**, *44*, 155−172.

(10) Abdullaev, F. I. Cancer chemopreventive and tumoricidal properties of saffron (*Crocus sativus L*). *Exp. Biol. Med.* **2002**, *227*, 20−25.

(11) Tarantilis, P. A.; Morjani, H.; Polissiou, M.; Manfait, M. Inhibition of growth and induction of differentiation of promyelocytic leukemia (HL-60) by catotenoids from *Crocus sativus* L. *Anticancer Res.* **1994**, *14*, 1913−1918.

(12) Zsila, F.; Bikadi, Z.; Simonyi, M. Further insight into the molecular vasis of carotenoid-albumin interactions: circular dichroism and electronic absorption study on different crocetin-albumin complexes. *Tetrahedron Asymm.* **2002**, *13*, 273−283.

(13) Zsila, F.; Bikadi, Z.; Simonyi, M. Induced chirality upon crocetin binding to human serum albumin: origin and nature. *Tetrahedron Asymm.* **2001**, *12*, 3125−3137.

(14) Sugio, S.; Kashima, A.; Mochizuki, S.; Noda, M.; Kobayashi, K. Crystal structure of human serum albumin at 2.5 Å resolution. *Protein Eng.* **1999**, *12*, 439−446.

(15) Carter, D. C.; Ho, J. X.; Structure of Serum Albumin. *Adv. Protein Chem.* **1994**, *45*, 153−203.

(16) Peters, T. All about albumin. In *Biochemistry, Genetics and Medical Applications*; Academic Press: San Diego, 1996.

(17) He, H. M.; Carter, D. C. Atomic structure and chemistry of human serum albumin. *Nature* **1992**, *358*, 209−215.

(18) Peters, T. Serum albumin. *Adv. Protein Chem.* **1985**, *37*, 161−245.

(19) Curry, S.; Brick, P.; Frank, N. P. Atomic structure and chemistry of human serum albumin. *Biochim. Biophys. Acta* **1999**, *1441*, 131−140.

(20) Petitpas, I.; Grune, T.; Battacharya, A. A.; Curry, S. Crystal structure of human serum albumin complexed with monounsaturated and polyunsaturated fatty acids. *J. Mol. Biol.* **2001**, *314*, 955−960.

(21) Grelamo, E. L.; Silva, C. H.; Imasato, H.; Tabak, M. Interaction of bovine (BSA) and human (HSA) serum albumins with ionic surfactants: spectroscopy and modelling. *Biochim. Biophys. Acta* **2002**, *1594*, 84−99.

(22) Chuang, V. T. G.; Otagiri, M. A 7-nitro-1,4-benzodiazepine that is unable to bind to indole-benzodiazepine site of human serum albumin. *Biochim. Biophys. Acta* **2001**, *1546*, 337−345.

(23) Painter, L.; Harding, M. M.; Beeby, P. J. Synthesis and interaction with human serum albumin of the first 3,18-disubstituted derivative of bilirubin. *J. Chem. Soc., Perkin Trans. 1* **1998**, *118*, 3041−4044.

(24) Krimm, S.; Bandekar, J.; Vibrational spectroscopy and conformation of peptides, polypeptides and proteins. *Adv. Protein Chem.* **1986**, *38*, 181−364.

(25) Tarantilis, P. A.; Beljebbar, A.; Manfait, M.; Polissiou, M. FT-IR, FT-Raman spectroscopic study of carotenoids from saffron (*Crocus sativus L.*) and some derivatives. *Spectrochim. Acta, Part A* **1998**, *54*, 651−657.

(26) Tepe, B.; Sokmen, M.; Askin, Akpulat, H.; Daferera, D.; Polissiou, M.; Sokmen, A. Antioxidant activity of the essential oils of *Thymus sipyleus* subsp. *Sipyleus* var. *sipyleus* and *Thymus sipyleus* subsp. *Sipyleus* var. *rosulans*. *J. Food Eng.* **2005**, *66*, 447−454.

(27) Jiménez-Escrib, A.; Jiménez- Jiménez, I.; Sánchez-Moreno, C.; Saura-Calixto, F. Evaluation of free radical scavenging of dietary carotenoids by the stable radical 2,2-diphenyl-1-picrylhydrazyl. *J. Sci. Food Agric.* **2000**, *80*, 1686−1690.

(28) Painter, L.; Harding, M. M.; Beeby, P. J. Synthesis and interaction with human serum albumin of the first 3,18-disubstituted derivative of bilirubin. *J. Chem. Soc., Perkin Trans. 1* **1998**, *18*, 3041−3044.

(29) Harding, S. E.; Chardhry, B. Z. *Protein-Ligand Interactions: structure and spectroscopy*; Oxford University Press: Oxford, 2001.

(30) Krimm, S.; Bandekar, J. Vibrational spectroscopy and conformation of peptides, polypeptides and proteins. *Adv. Protein Chem.* **1986**, *38*, 181−364.

(31) Ahmed, Ouamer, A.; Mangier, E.; Diamantoglou, S.; Rouillon, R.; Carpentier, R.; Tajmir Riahi, H. A. Effects of organic and inorganic polyamine cations on the structure of human serum albumin. *Biopolymers* **2004**, *73*, 503−509.

(32) Byler, D. M.; Susi, A. Examination of the secondary structure of proteins by deconvoluted FT-IR spectra. *Biopolymers* **1986**, *25*, 469−487.
(33) Ahmed, A.; Tajmir-Riahi, H. A.; Carpentier, R. A quantitative secondary structure analysis of the 33 kDa extrinsic polypeptide of the photosystem II by FT-IR spectroscopy. *FEBS Lett.* **1995**, *363*, 65−68.
(34) Stephanos, J. J.; Farina, S. A.; Addison, A. W. Iron ligand recognition by monomeric hemoglobins. *Biochim. Biophys. Acta* **1996**, *1295*, 209−221.
(35) Stephanos, J. J. Drug-Protein-Interactions: Two-Site Binding of Heterocyclic Ligands to a Monomeric Hemoglobin. *J. Inorg. Biochem.* **1996**, *62*, 155−169.
(36) Holloway, G. M.; Gainer, J. L. The carotenoid crocetin enhances pulmonary oxygenation. *J. Appl. Physiol.* **1988**, *65*, 683−683.
(37) Krinsky, N. I.; Yeung, K. J. Carotenoid radical interactions. *Biochem. Biophys. Res. Commun.* **2003**, *305*, 754−760.
(38) Roginsky, V.; Lissi, E. A. Review of methods to determine chain-breaking antioxidant activity in food. *Food Chem.* **2005**, *92*, 235−254.
(39) Boulkanz, L.; Balcar, N.; Baron, M. H. FT-IR analysis for structural characterisation of albumin absorbed on the reversed-phase support RP-C6. *Appl. Spectrosc.* **1995**, *49*, 1737−1746.
(40) Bramanti, E.; Benedetti, E. Determination of the secondary structure of isomeric forms of human serum albumin by a particular frequency deconvolution procedure to Fourier transform IR analysis. *Biopolymers* **1996**, *38*, 639−653.
(41) Gaudreu, S.; Neault, J. F.; Tajmir-Riahi, H. A. Interaction of AZT with human serum albumin studied by capillary electrophoresis, FT-IR and CD spectroscopic methods. *J. Biomol. Struct. Dyn.* **2002**, *19*, 1007−1014.
(42) Neault, J. F.; Novetta-Delen, A.; Arakawa, H.; Malonga, H.; Tajmir-Riahi, H. A. The effect of aspirin −HSA complexation on the protein secondary structure. *Can. J. Chem.* **2000**, *78*, 291−296.
(43) Xie, M.-X.; Long, M.; Liu, Y.; Qin, C.; Wang, Y.-D. Characterization of the interaction between human serum albumin and morin. *Biochim. Biophys. Acta* **2006**, *53*, 77−82.
(44) Li, Y.; He, W. Y.; Dong, Y. M.; Sheng, F.; Hu, Z. D. Human serum albumin interaction with formononetin studied using fluorescence anisotropy, FT-IR spectroscopy and molecular modeling methods. *Bioorg. Med. Chem.* **2006**, *14*, 1431−1436.
(45) Kanakis, C. D.; Tarantilis, P. A.; Polissiou, M. G.; Diamantoglou, S.; Tajmir-Riahi, H. A. Antioxidant flavonoids bind human serum albumin. *J. Mol. Struct.* **2006**, *798*, 69−74.
(46) Ahmed, Ouamer, A.; Marty, R.; Tajmir-Riahi, H. A. Human serum albumin complexes with chlorophyll and chlorophyllin. *Biopolymers* **2005**, *77*, 129−136.
(47) Lin, S.-Y.; Li, M.-J.; Wei, Y.-S. Ethanol or/and captopril-induced precipitation and secondary conformational changes of human serum albumin. *Spectrochim. Acta, Part A* **2004**, *60*, 3107−3111.
(48) Dean, J. D. Flavone: The molecular and mechanistic study of how a simple flavonoid protects DNA from oxidative damage. Ph.D. thesis, East Tennessee State University, 2003.
(49) Kragh-Hansen, U. Structure and ligand binding properties of human serum albumin. *Dan. Med. Bull.* **1990**, *37*, 57−84.
(50) Dufour, C.; Dangles, O. Flavonoid-serum albumin complexation: determination of binding constants and binding sites by fluorescence spectroscopy. *Biochim. Biophys. Acta* **2005**, *1721*, 164−173.
(51) Zsila, F.; Bikádi, Z.; Simonyi, M. Probing the binding of the flavonoid quercetin to human serum albumin by circular dichroism, electronic absorption spectroscopy and molecular modelling methods. *Biochem. Pharmacol.* **2003**, *65*, 447−456.

Received for review September 15, 2006. Revised manuscript received November 27, 2006. Accepted December 7, 2006. This work was supported by grants from the Natural Sciences and Engineering Research Council of Canada (NSERC), the Agricultural University of Athens, and IKY (State Scholarships Foundation of Greece).

JF062638L